



2006

Clustering of Cr in GaN nanotubes and the onset of ferrimagnetic order

Q. Wang

Virginia Commonwealth University

Q. Sun

Virginia Commonwealth University

Puru Jena

Virginia Commonwealth University, pjena@vcu.edu

Y. Kawazoe

Tohoku University

Follow this and additional works at: http://scholarscompass.vcu.edu/phys_pubs

 Part of the [Physics Commons](#)

Wang, Q., Sun, Q., Jena, P., et al. Clustering of Cr in GaN nanotubes and the onset of ferrimagnetic order. *Physical Review B*, 73, 205320 (2006). Copyright © 2006 American Physical Society.

Downloaded from

http://scholarscompass.vcu.edu/phys_pubs/82

This Article is brought to you for free and open access by the Dept. of Physics at VCU Scholars Compass. It has been accepted for inclusion in Physics Publications by an authorized administrator of VCU Scholars Compass. For more information, please contact libcompass@vcu.edu.

Clustering of Cr in GaN nanotubes and the onset of ferrimagnetic order

Q. Wang,¹ Q. Sun,¹ P. Jena,¹ and Y. Kawazoe²

¹*Department of Physics, Virginia Commonwealth University, Richmond, Virginia 23284-2000, USA*

²*Institute for Materials Research, Tohoku University, Sendai, 980-8577 Japan*

(Received 10 April 2006; published 10 May 2006)

A comprehensive theoretical study of the structure and magnetic properties of Cr-doped GaN nanotubes yields some interesting and unexpected results: (1) A single wall GaN nanotube constructed from the GaN wurtzite crystal relaxes to a carbon-like zigzag SWNT structure and remains stable at 300 K, while a multiwall GaN nanotube retains its original wurtzite form. (2) Cr atoms prefer to form clusters and the underlying magnetism depends on the degree of clustering. (3) The coupling between two Cr atoms mediated by the neighboring N is ferromagnetic, but changes to ferrimagnetic as the cluster grows. These results are based on spin polarized density functional theory with exchange and correlation potential approximated by both the generalized gradient approximation and the local spin density approximation + U methods.

DOI: [10.1103/PhysRevB.73.205320](https://doi.org/10.1103/PhysRevB.73.205320)

PACS number(s): 75.75.+a, 36.40.Cg, 73.22.-f, 75.50.Pp

I. INTRODUCTION

The discovery of dilute magnetic semiconductors has given rise to a great deal of experimental and theoretical activities¹⁻⁶ aimed at finding and understanding of materials that can be ferromagnetic at room temperature. Among these, the most widely studied materials are Mn doped GaN and ZnO in thin film and bulk forms. However, many of the reported results have been controversial and are known to depend upon sample conditions. Recently emphasis has shifted to one-dimensional (1D) and quasi-1D materials as the next generation building blocks for electronic and optical devices. These include nanowires (NWs), nanotubes (NTs), and nanohole (NH) arrays. For example, GaN NTs have been successfully synthesized,^{7,8} and their formation mechanism,⁹ stability and electronic properties^{10,11} have been studied. The synthesis of the perfect single crystal GaN NTs (Ref. 8) opens up new possibilities for fabricating GaN NT-based new functional materials for spintronics devices by introducing transition metal ions (carriers) and taking advantage of its spin degree of freedom. Unlike the nanowires, NTs offer flexibility in doping because the dopants can occupy the interior as well as the exterior surface sites of the tube. In addition, NTs have lower mass density, high porosity, and very large surface to weight ratio.

In this paper, we present the first theoretical study of the structure and magnetic properties of Cr-doped GaN NTs as a function of Cr concentration. The advantage of Cr is that the small energy gap between the $3d$ and $4s$ orbitals allows it to exist in different oxidation states, namely, 0, +2, +3, and +6, which can be used to tune the structure and magnetic properties of a Cr-doped material. In particular, unlike Mn-doped GaN, Cr-doped GaN materials are found to be ferromagnetic (FM) irrespective of whether they exist as a crystal,⁴ thin films,⁵ or NWs (Ref. 6). Using density functional theory and different levels of correlation corrections [generalized gradient approximation (GGA) and local spin density approximation + U (LSDA+ U)], we have studied the preferred sites of Cr atoms and their magnetic coupling. We show that the coupling between two Cr atoms is FM whether it is a single-

wall nanotube (SWNT) or multiwall nanotube (MWNT). However, as the concentration increases, Cr atoms prefer to cluster and the coupling changes to ferrimagnetic. Our computational procedures and results are discussed in the following.

II. THEORETICAL METHOD

The GaN NT has been generated from a $(7 \times 7 \times 3)$ GaN supercell having wurtzite crystal structure and experimental lattice constants ($a=3.189$ Å, $c=5.185$ Å).⁸ The atoms from the outside and inside areas of the two circles [see Fig. 1(a)] were removed and replaced with a vacuum space. The NT supercell thus created contains 54 Ga atoms and 54 N atoms with a vacuum space of 12.756 Å and 13.097 Å along the $[10\bar{1}0]$ $[01\bar{1}0]$ directions, respectively. It extends to infinity along the $[0001]$ direction through the repetition of the periodic supercell [see Fig. 1(b)]. The vacuum space is large enough to ensure that the interactions from the atoms in the neighboring supercells are negligible. This NT has a polygonal periphery with the diameters of 9.760 Å for the outer shell and 7.808 Å for the inner shell when viewed from the central tube axis (the $[0001]$ direction) [see Fig. 2(a)].

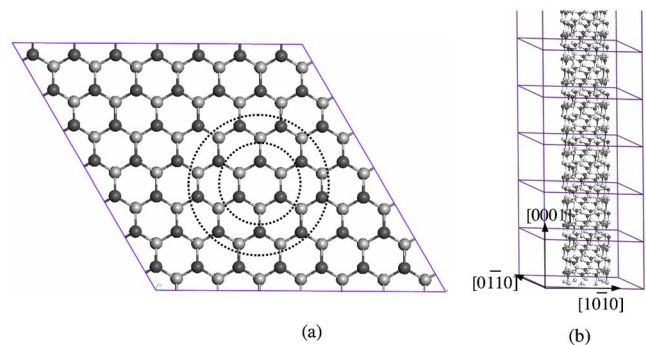


FIG. 1. (Color online) (a) Top view of a $7 \times 7 \times 3$ GaN supercell having wurtzite structure. (b) GaN-NT supercell ($\text{Ga}_{54}\text{N}_{54}$) which extends to infinite length along the $[0001]$ direction.

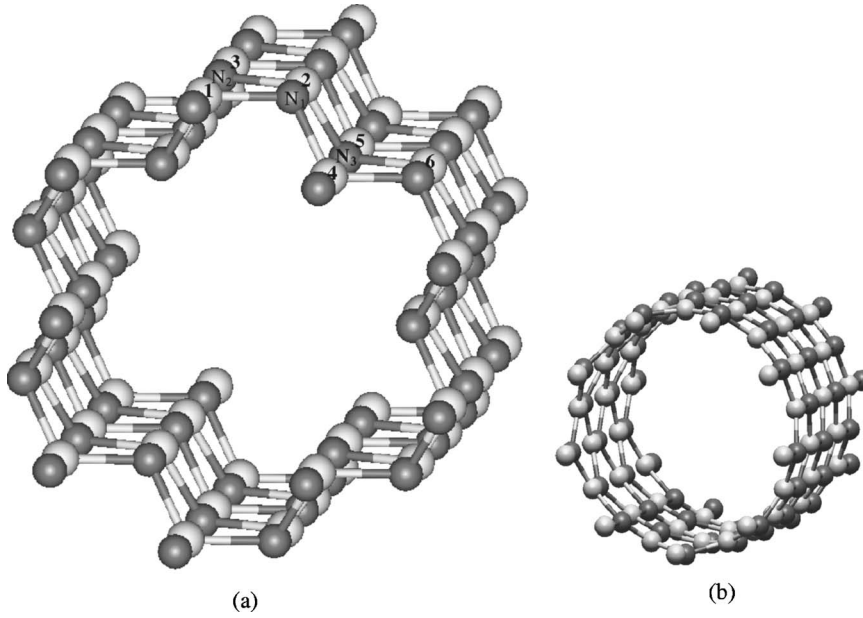


FIG. 2. Schematic representation of the initial (a) and the optimized (b) GaN NT supercell ($\text{Ga}_{54}\text{N}_{54}$). The lighter spheres are Ga and the darker spheres are N.

To study the magnetic coupling between Cr atoms in the NT, we first replaced two Ga atoms with two Cr atoms. This corresponds to a 3.7% Cr doping concentration. There are many ways this substitution can be achieved, depending upon the sites where Cr atoms are distributed. It has been well established that Cr atoms prefer to cluster around N and reside in the outermost surface layer in GaN thin films⁵ and NWs (Ref. 6). Consequently, we have chosen six configurations to simulate the different Cr-Cr and Cr-N distances as well as Cr-N-Cr bond angles. These are specified in Table I and Fig. 2(a). To study the preferred magnetic coupling, we have calculated the total energies for both FM and antiferromagnetic (AFM) states with full geometry optimization for all the configurations. To study the dependence of magnetic coupling between Cr atoms on the thickness of GaN NTs, we generated a MWNT from a $9 \times 9 \times 2$ GaN supercell and changed the doping concentration of Cr to 2.1% by replacing two Ga atoms with two Cr atoms. The effect of Cr concentration was also taken into account by increasing the number of Cr atoms in the supercell as well as the supercell size.

The calculations of total energies and forces, and optimizations of geometry of the supercell with and without Cr substitution have been carried out using spin polarized density functional theory (DFT) and Perdew and Wang 91

(PW91) functional¹² for GGA for exchange and correlation potential. A plane-wave basis set and the projector augmented wave (PAW) potentials^{13,14} for Ga, N, and Cr as implemented in the Vienna *ab initio* Simulation Package¹⁵ (VASP) were employed. The energy cutoff was set at 330 eV and the convergence in energy and force was set to 10^{-4} eV and 10^{-3} eV/Å, respectively. To explore the effect of the Coulomb correlation on the electronic structure and magnetic coupling of the Cr-doped GaN NTs, LSDA+U calculations^{16,17} also have been performed.

III. RESULTS AND DISCUSSIONS

We begin our discussion with results of the electronic structure of the pure GaN NT. The geometry optimization was carried out by allowing the atomic coordinates of all the atoms in the $\text{Ga}_{54}\text{N}_{54}$ supercell to relax without any symmetry constraint. It was found that the initial polygon structure of the NT in Fig. 2(a) transformed into a perfect cylindrical tube—SWNT with the radius of 4.92 Å, see Fig. 2(b). It is very interesting to note that this optimized GaN SWNT has the same structural feature as the carbon (9, 0) SWNT, which has a radius of 3.55 Å. The relaxed Cr-N bond length is found to be 1.846 Å along the [0001] and 1.869 Å approxi-

TABLE I. The energy difference ΔE between AFM and FM states (in eV), the relative energy $\Delta \epsilon$ (in eV) calculated with respect to the ground state configuration III, the average magnetic moments (in μ_B) at Cr and that arising from Cr 3d orbitals, and the optimized Cr-Cr and the nearest Cr-N distances (in Å) for the GaN SWNT corresponding to the supercell $\text{Ga}_{52}\text{Cr}_2\text{N}_{54}$.

Configurations	ΔE	$\Delta \epsilon$	μ_{Cr}	$\mu_{\text{Cr-3d}}$	Coupling	$d_{\text{Cr-Cr}}$	$d_{\text{Cr-N}}$
I(Ga1,Ga2)	0.104	0.045	2.770	2.676	FM	2.997	1.807
II(Ga1,Ga3)	-0.017	0.302	2.574	2.489	AFM	5.139	1.836
III(Ga2,Ga6)	0.245	0.000	2.674	2.587	FM	3.508	1.827
IV(Ga2,Ga5)	0.109	0.046	2.779	2.691	FM	3.009	1.807
V(Ga3,Ga5)	0.251	0.001	2.669	2.583	FM	3.505	1.829
VI(Ga4,Ga5)	-0.019	0.301	2.573	2.487	AFM	5.139	1.836

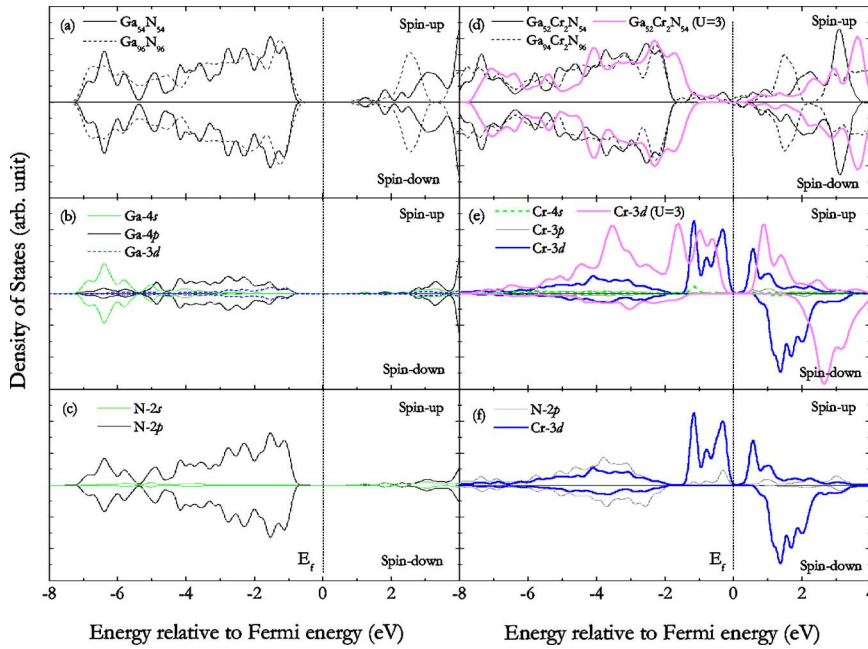


FIG. 3. (Color online) (a) Total DOS corresponding to pure $\text{Ga}_{54}\text{N}_{54}$ NT (solid line) and $\text{Ga}_{96}\text{N}_{96}$ NT (dashed line); (b) partial spin DOS of Ga in $\text{Ga}_{54}\text{N}_{54}$; (c) partial spin DOS of N in $\text{Ga}_{54}\text{N}_{54}$; (d) total DOS of Cr-doped GaN-NT for $\text{Ga}_{52}\text{Cr}_2\text{N}_{54}$ (solid line), $\text{Ga}_{94}\text{Cr}_2\text{N}_{96}$ (dashed line), and LSDA+U result for $\text{Ga}_{52}\text{Cr}_2\text{N}_{54}$ (lighter magenta solid line); (e) partial spin DOS of Cr in $\text{G}_{52}\text{Cr}_2\text{N}_{54}$; (f) partial spin DOS of Cr $3d$ and N $2p$ in $\text{Ga}_{52}\text{Cr}_2\text{N}_{54}$.

mately along the $[10\bar{1}0]$ directions, which contracted by -7.05% and -3.61% , respectively, as compared with those in the bulk. The nearest Ga-Ga and N-N distances are 3.085 \AA and 3.118 \AA , respectively. The total energy of the relaxed supercell was found to be 35.956 eV lower than the unrelaxed one, corresponding to an energy gain of $0.666 \text{ eV/Ga-N dimer}$, which is much larger than that in Cr-doped GaN nanowires.⁶ The total electronic density of states (DOS) for spin-up and spin-down electrons corresponding to the pure GaN SWNT supercell is plotted in Fig. 3(a). The partial spin DOS for Ga and N atoms are given in Figs. 3(b) and 3(c), respectively. They show that the valance band is essentially composed of N $2p$ with small contributions from the orbitals of Ga atom. The conduction band is made up of Ga $4p$, $4s$, and N $2p$ states with negligible contributions from Ga $3d$ and N $2s$. The DOS for spin-up and spin-down electrons are identical and the Fermi level is located in the gap region, indicating that GaN NT has semiconducting features. The band gap is found to be 2.31 eV , which is comparable to the calculated value of 2.2 eV for the $(8, 0)$ GaN SWNT (Ref. 11).

We next discuss the magnetic coupling between the two Cr atoms in GaN NT. We started the calculations with the initial geometry as shown in Fig. 2(a), since it is not clear if the NT's geometry would change from the initial polygon structure to the SWNT, once Cr is doped. The main results are summarized in Table I. In the first column, we list the six configurations by specifying the Ga atoms that were replaced by Cr as shown in Fig. 2(a). There are three kinds of configurations: (1) Both Cr atoms are on the outmost shell (configurations I, II, III); (2) one Cr atom is on the outmost shell while another Cr is in the inner shell (configurations IV, V); and (3) both Cr atoms are in the inner shell forming nearest neighbors (configuration VI). Total energy calculations with full geometry optimization have been carried out for all the six configurations for both FM and AFM spin alignments to determine the preferred magnetic ground state.

The energy difference ΔE between the AFM and FM states [$\Delta E = E(\text{AFM}) - E(\text{FM})$] corresponding to the relaxed states are listed in the second column of Table I. Configuration III was found to be the ground state with the FM state lying 0.245 eV lower in energy than the AFM state. Using the total energy of the ground state configuration as a reference, the relative energies $\Delta \varepsilon$ calculated with respect to the other five configurations are given in Table I. Comparing the relative energies in the third column, we note that configurations I and IV, configurations II and VI, and configurations III and V are respectively energetically degenerate. It is also important to note that the initial geometries of all the configurations change substantially following the relaxation. The initial six different configurations yield three final different configurations upon geometry optimizations: configurations I and IV, II and VI, and III and V have, respectively, the same structure after relaxation. The geometries of all these three configurations are tubular with almost the same radius as that of the pure GaN SWNT and similar to that for the carbon $(9, 0)$ SWNT. In the last three columns of Table I, we have given the preferred magnetic coupling, the distances between the two Cr atoms and that between Cr and the nearest N. Once again it was found that the relaxation in this Cr-doped GaN SWNT is quite large. For instance, in the ground state configuration, the Cr-N bond length is calculated to be 1.827 \AA along the $[0001]$ and 1.843 \AA approximately along the $[10\bar{1}0]$ directions, which contracted by -8.01% and -4.90% , respectively, as compared with those in the bulk. The surface relaxation has resulted in a large change of the Cr-Cr distance, from 3.189 \AA to 3.408 \AA .

The total DOS corresponding to the ground state of configuration III is shown in Fig. 3(d). The partial DOS of the Cr atom and the partial DOS of the Cr $3d$ and the nearest N $2p$ states are plotted in Figs. 3(e) and 3(f), respectively. Note that the DOS for spin-up and spin-down states are not identical any more, the energy gap has disappeared, and the Cr $3d$ majority states dominate the DOS at the Fermi energy.

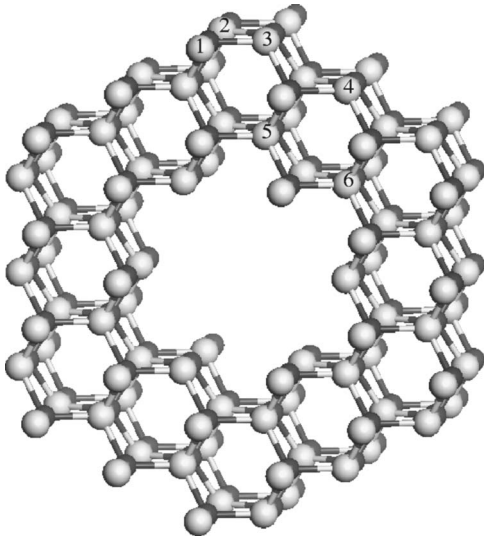


FIG. 4. Schematic representation of the GaN MWNT supercell ($\text{Ga}_{96}\text{N}_{96}$). The lighter spheres are Ga and the darker spheres are N. The atoms occupying sites marked 1 and 2 are along the $[0001]$ direction.

Figure 3(f) shows that there is a visible overlap between Cr $3d$ and N $2p$ states which mediate the FM coupling of the Cr atoms. In particular, the majority N $2p$ states are more hybridized with Cr $3d$ orbitals than the minority states. This results in a polarized magnetic moment of the N atom. The calculations of the magnetic moment located on each Cr atom have been carried out self-consistently. It was found that, in the ground state, the magnetic moments located on the two Cr atoms are $2.669\mu_B$ and $2.678\mu_B$ and mainly arise from the Cr $3d$ orbitals ($2.583\mu_B$ and $2.591\mu_B$, respectively). The partial DOS of Cr in Fig. 3(e) shows this feature clearly. The neighboring N atom is polarized antiferromagnetically and carries a magnetic moment of $-0.18\mu_B$. The average magnetic moments at Cr and that arising from Cr $3d$ orbitals are given for all the configurations in the fourth and fifth columns of Table I, respectively. It shows that the Cr atoms carry slightly different moments ranging from $2.57\mu_B$ to $2.80\mu_B$ since they occupy different sites in the NT, and mainly come from the Cr $3d$ orbitals ($2.49\mu_B$ to $2.69\mu_B$).

Since the stability of the structures that we described above at finite temperature is crucial for fabricating devices, we performed the finite-temperature *ab initio* molecular dynamics (MD) calculations¹⁸ on the pure GaN SWNT. It was

found that the tubular structure at $T=0$ K remains stable at 300 K after 2000 time steps with the time step of 1.0 fs. No significant distortions have been found.

To study the effects of the thickness of the NT wall and the Cr concentration on the magnetic coupling between Cr atoms, we performed additional calculations for a GaN MWNT. This was generated from a $(9 \times 9 \times 2)$ GaN supercell following the same procedure as discussed for the GaN SWNT. The MWNT supercell contains a total of 192 atoms ($\text{Ga}_{96}\text{N}_{96}$) with a diameter of 7.808 Å for the innermost wall and a diameter of 16.259 Å for the outermost wall, as shown Fig. 4, and has a vacuum space of about 13 Å along the $[1010]$ and $[0110]$ directions. The length of the NT extends to infinity along the $[0001]$ direction through the supercell repetition. We have replaced a pair of the nearest neighbor Ga atoms with two Cr atoms in four different sites to study their magnetic coupling. These replacements resulted in four configurations, which are specified in Table II (see Fig. 4) and correspond to a 2.1% Cr doping concentration ($\text{Ga}_{94}\text{Cr}_2\text{N}_{96}$). The calculations for this MWNT with and without Cr doping have been carried out the same way as described for the SWNT. It was found that the relaxation energy for the pure $\text{Ga}_{96}\text{N}_{96}$ NT is 0.225 eV/Ga-N dimer, which is similar to that in GaN nanowires,⁶ but is only about one third of that for the GaN SWNT. The structural relaxation, consequently, is much less and the optimized structure is very similar to the initial one. Therefore, the morphology of the GaN MWNT is different from that of SWNT. The relaxed Ga-N bond length for the pure MWNT on the surface of the outermost wall along the $[0001]$ direction is about 1.868 Å. The bond length of Ga-N dimer which is approximately along the $[1010]$ direction is 1.892 Å. The total DOS for spin-up and spin-down electrons of this pure NT is plotted in Fig. 3(a). It shows the same semiconducting feature as we found in the GaN SWNT. For the Cr-doped GaN NT, $\text{Ga}_{94}\text{Cr}_2\text{N}_{96}$, the results are summarized in Table II and the total DOS is plotted in Fig. 3(d). The FM nature is still preserved. It was found that configuration I is the ground state with the FM state lying lower in energy by 0.074 eV than that in the AFM state. The other three configurations are respectively 0.214, 0.882, and 1.132 eV higher in energy than the ground state configuration I. Therefore, it is apparent that the FM coupling between the Cr atoms is not affected by the thickness of GaN NT. Although the AFM state is more stable than the FM one for configuration III, due to a very large Cr-N bond length contraction (-15.4%) which drives the AFM coupling, it is 0.882 eV higher in energy than the ground state.

TABLE II. The energy difference ΔE (in eV) between AFM and FM states, the relative energy $\Delta\varepsilon$ (in eV) calculated with respect to the ground state configuration I, the magnetic moments (in μ_B) at each Cr, and the optimized Cr-Cr and the nearest Cr-N distances (in Å) for the GaN MWNT corresponding to the supercell $\text{Ga}_{94}\text{Cr}_2\text{N}_{96}$.

Configurations	ΔE	$\Delta\varepsilon$	μ_{Cr1}	μ_{Cr2}	$d_{\text{Cr-Cr}}$	$d_{\text{Cr-N}}$
I(Ga2,Ga3)	0.074	0.000	2.606	2.657	3.017(-5.15%)	1.826
II(Ga3,Ga4)	0.118	0.214	2.556	2.785	3.270(2.57%)	1.923
III(Ga4,Ga5)	-0.041	0.882	2.011	-2.092	2.698(-15.4%)	1.786
IV(Ga5,Ga6)	0.318	1.132	2.493	2.493	3.246(1.79%)	1.847

TABLE III. The energy difference ΔE between AFM and FM states (in eV), the average magnetic moments at Cr sites (in μ_B) calculated using LSDA+U method for $\text{Ga}_{52}\text{Cr}_2\text{N}_{54}$ and $\text{Ga}_{94}\text{Cr}_2\text{N}_{96}$ supercells and compared with GGA results.

$\text{Ga}_{52}\text{Cr}_2\text{N}_{54}$	GGA	$U=2$	$U=3$	$U=4$	$U=5$	$U=6$
ΔE	0.245	0.212	0.188	0.172	0.161	0.153
μ_{Cr}	2.674	2.844	2.930	3.013	3.086	3.159
μ_{N}	-0.183	-0.216	-0.229	-0.243	-0.253	-0.263
$\text{Ga}_{94}\text{Cr}_2\text{N}_{96}$	GGA	$U=2$	$U=3$	$U=4$	$U=5$	$U=6$
ΔE	0.074	0.061	0.058	0.063	0.065	0.066
μ_{Cr}	2.632	2.798	2.910	3.003	3.089	3.171
μ_{N}	-0.163	-0.185	-0.202	-0.219	-0.242	-0.268

To further confirm that the calculated ferromagnetism in Cr-doped GaN NTs is not a consequence of the approximation to exchange and correlation potential, we have employed the LSDA+U method. This replaces the Coulomb interaction among the localized electrons (e.g., transition metal d) by statically screened parameters U and J . We have taken into account the Coulomb correction U for Cr $3d$ electrons in the calculations for the ground state configurations of both the SWNT and the MWNT. We varied U from 2 eV to 6 eV, treating it as a parameter, in order to find out how the magnetic coupling is affected by the strength of the Coulomb correlation. The exchange interaction parameter J was taken to be 0.87 eV which was used in some previous calculations.^{19,20} The main results for both $\text{Ga}_{52}\text{Cr}_2\text{N}_{54}$ and $\text{Ga}_{94}\text{Cr}_2\text{N}_{96}$ are summarized in Table III. The total DOS for $\text{Ga}_{52}\text{Cr}_2\text{N}_{54}$ and the partial DOS for Cr at $U=3$ eV are plotted in Figs. 3(d) and 3(e), respectively. The Coulomb correlation effects are obvious: The Cr $3d$ spin splitting is enlarged and the local magnetic moment is increased. The value of the local magnetic moment at the Cr site increases with the Coulomb U : from $2.844\mu_B$ ($U=2$) to $3.159\mu_B$ ($U=6$) in $\text{Ga}_{52}\text{Cr}_2\text{N}_{54}$, and from $2.798\mu_B$ ($U=2$) to $3.122\mu_B$ ($U=6$) in $\text{Ga}_{94}\text{Cr}_2\text{N}_{96}$ NT. The main effect of the correction U on the DOS of the Cr-doped GaN NTs, shown in Figs. 3(d) and 3(e), is a downward shift of the Cr $3d$ spin-up states and an upward shift of the spin-down states. The Cr $3d$ partial spin DOS at the Fermi level E_F is suppressed in the LSDA+U calculation. However, it is important to note that the introduction of U over quite a large range (2–6 eV) does not change the magnetic coupling between Cr atoms in both the SWNT and the MWNT, as given in Table III. The FM states always are lower in energy than the AFM states, irrespective of how large the U we chose. This shows the high stability of the FM coupling between Cr atoms in GaN NTs. The mechanism of driving this FM coupling in Cr-doped GaN NTs is found to be similar to that in thin films and nanowires, namely, it is mediated by the hybridization of Cr $3d$ and N $2p$ orbitals.

Finally, we have investigated whether the coupling between Cr atoms remains FM when four Ga atoms in the supercell are replaced by Cr. We chose a longer GaN SWNT supercell which was generated from a $7 \times 7 \times 4$ GaN supercell containing a total of 144 atoms ($\text{Ga}_{72}\text{N}_{72}$). We replaced

two pairs of Ga atoms with Cr atoms at different sites and have carried out extensive search for the most favored geometric and magnetic configuration. Especially, we paid close attention to the sites where the two pairs of Ga atoms line up along [0001] direction and are 10.37 Å from each other (configuration I) as well as the sites where the four Ga atoms form nearest neighbors (configuration II). The total energy calculations clearly showed that Cr atoms prefer to cluster and configuration II is the most stable structure lying 1.13 eV lower in energy than configuration I. For this ground state configuration, calculations were carried out for different spin alignments, namely ($\uparrow\uparrow\uparrow\uparrow$), ($\uparrow\downarrow\uparrow\uparrow$), ($\uparrow\uparrow\downarrow\uparrow$), ($\uparrow\uparrow\uparrow\downarrow$), ($\uparrow\downarrow\downarrow\downarrow$), and ($\uparrow\uparrow\downarrow\downarrow$). It was found that the energetically most favorable spin state is ferrimagnetic coupling ($\uparrow\downarrow\uparrow\uparrow$) which has a total magnetic moment of $4.02\mu_B$. The magnetic moment on each atom is (1.774, -2.830, 2.559, 2.243) μ_B . This spin state is 0.055, 0.062, 0.259, 0.097, and 0.152 eV lower in energy than ($\uparrow\uparrow\uparrow\uparrow$), ($\uparrow\uparrow\downarrow\uparrow$), ($\uparrow\uparrow\uparrow\downarrow$), ($\uparrow\downarrow\downarrow\downarrow$), and ($\uparrow\uparrow\downarrow\downarrow$) states, respectively. The results indicate that the magnetic interaction in Cr-doped GaN NTs is short ranged and the Cr atoms have a strong tendency to form embedded clusters. In addition, the ferrimagnetic state is energetically preferred over the FM state for the Cr clusters larger than two atoms—in agreement with recent calculations in bulk systems.^{21–23}

IV. SUMMARY

In conclusion, we have studied the electronic and magnetic properties of Cr-doped GaN NTs using GGA as well as LSDA+U methods. We have shown that GaN SWNT which was generated from GaN wurtzite crystalline structure along [0001] direction has the same structural feature as carbon SWNT due to large relaxation and is stable at room temperature. FM coupling is energetically favorable in Cr-doped GaN NTs irrespective of the NT's thickness as long as the Cr concentration remains small. The FM coupling results from the hybridization of the N $2p$ and the Cr $3d$ states. It was found that as the wall thickness of GaN NT increases, the structural relaxations become smaller, and Cr atoms prefer to occupy the sites on the outer wall surface. This is because the stress produced on the outer wall is smaller than that in the inner wall. However, as the size of the NT becomes larger,

this difference between the outer wall and the inner wall would become smaller. Therefore, we can expect that as the NT size reaches some critical value, the doped Cr atoms would equally occupy both outer wall sites and inner wall sites. Thus, a tubular sandwich structure could result. The magnetic inner wall provides additional advantage for many applications as compared to GaN NWs. In addition, Cr atoms have a tendency to cluster as the concentration increases and the magnetic coupling changes to ferrimagnetic. The cancellation between individual Cr moments thus will lead to a small average moment per Cr atom—an effect that is widely

seen in many DMS materials even though the individual moments are quite large.

ACKNOWLEDGMENTS

The work was supported in part by a grant from the Office of Naval Research. The authors thank the staff of the Center for Computational Materials Science, the Institute for Materials Research, Tohoku University (Japan), for their continuous support of the HITACH SR8000 supercomputing facility.

-
- ¹H. Ohno, *Science* **281**, 951 (1998); T. Dietl, H. Ohno, F. Matsukura, J. Cibert, and D. Ferrant, *Science* **287**, 1019 (2000); H. Ohno, *Science* **291**, 840 (2001); Y. Matsumoto, M. Murakami, T. Shono, T. Hasegawa, T. Fukumura *et al.*, *Science* **291**, 854 (2001); S. A. Wolf, *Science* **294**, 1488 (2001).
- ²M. L. Reed, N. A. El-Masry, H. H. Stadelmaier, M. K. Rittums, M. J. Reed *et al.*, *Appl. Phys. Lett.* **79**, 3473 (2001); S. Dhar, O. Brandt, A. Trampert, L. Däweritz, K. J. Friedland *et al.*, *Appl. Phys. Lett.* **82**, 2077 (2003).
- ³J. König, H. H. Lin, and A. H. MacDonald, *Phys. Rev. Lett.* **84**, 5628 (2000); J. Schliemann and A. H. MacDonald, *Phys. Rev. Lett.* **88**, 137201 (2002); S. C. Erwin and A. G. Petukhov, *Phys. Rev. Lett.* **89**, 227201 (2002); Q. Wang, Q. Sun, P. Jena, and Y. Kawazoe, *Phys. Rev. Lett.* **93**, 155501 (2004).
- ⁴S. E. Park, H.-J. Lee, Y. C. Cho, S.-Y. Jeong, C. R. Cho *et al.*, *Appl. Phys. Lett.* **80**, 4187 (2002); M. Hashimoto, Y.-K. Zhou, M. Kanamura, and H. Asahi, *Solid State Commun.* **122**, 37 (2002); J. S. Lee, J. D. Lim, Z. G. Khim, Y. D. Park, S. J. Pearton *et al.*, *J. Appl. Phys.* **93**, 4512 (2003).
- ⁵Q. Wang, Q. Sun, P. Jena, J. Z. Yu, R. Note, and Y. Kawazoe, *Phys. Rev. B* **72**, 045435 (2005); H. X. Liu, S. Y. Wu, R. K. Singh, L. Gu, D. J. Smith *et al.*, *Appl. Phys. Lett.* **85**, 4076 (2004).
- ⁶Q. Wang, Q. Sun, P. Jena, and Y. Kawazoe, *Nano Lett.* **5**, 1587 (2005).
- ⁷J. Y. Li, X. L. Chen, Z. Y. Qiao, Y. G. Cao, and H. Li, *J. Mater. Sci. Lett.* **20**, 1987 (2001).
- ⁸J. Goldberger, R. He, Y. Zhang, S. Lee, H. Yan *et al.*, *Nature* (London) **422**, 599 (2003).
- ⁹Z. Liliental-Weber, Y. Chen, S. Ruvimov, and J. Washburn, *Phys. Rev. Lett.* **79**, 2835 (1997).
- ¹⁰S. M. Lee, Y. H. Lee, Y. G. Hwang, J. Elsner, D. Porezag, and T. Frauenheim, *Phys. Rev. B* **60**, 7788 (1999).
- ¹¹E. Durgun, S. Tongay, and S. Ciraci, *Phys. Rev. B* **72**, 075420 (2005).
- ¹²Y. Wang and J. P. Perdew, *Phys. Rev. B* **44**, 13298 (1991).
- ¹³G. Kresse and D. Joubert, *Phys. Rev. B* **59**, 1758 (1999).
- ¹⁴P. E. Blöchl, *Phys. Rev. B* **50**, 17953 (1994).
- ¹⁵G. Kresse and J. Furthmüller, *Phys. Rev. B* **54**, 11169 (1996).
- ¹⁶V. I. Anisimov, J. Zaanen, and O. K. Andersen, *Phys. Rev. B* **44**, 943 (1991).
- ¹⁷A. I. Lichtenstein, V. I. Anisimov, and J. Zaanen, *Phys. Rev. B* **52**, R5467 (1995).
- ¹⁸S. Nosé, *J. Chem. Phys.* **81**, 511 (1984).
- ¹⁹M. A. Korotin, V. I. Anisimov, D. I. Khomskii, and G. A. Sawatzky, *Phys. Rev. Lett.* **80**, 4305 (1998).
- ²⁰T. Tsujioka, T. Mizokawa, J. Okamoto, A. Fujimori, M. Nohara, H. Takagi, K. Yamaura, and M. Takano, *Phys. Rev. B* **56**, R15509 (1997).
- ²¹X. Y. Cui, J. E. Medvedeva, B. Delley, A. J. Freeman, N. Newman, and C. Stampfl, *Phys. Rev. Lett.* **95**, 256404 (2005).
- ²²L. Bergqvist, O. Eriksson, J. Kudrnovsky, V. Drchal, P. Korzhavyi, and I. Turek, *Phys. Rev. Lett.* **93**, 137202 (2004).
- ²³K. Sato, W. Schweika, P. H. Dederichs, and H. Katayama-Yoshida, *Phys. Rev. B* **70**, 201202(R) (2004).